

Extreme ultraviolet spectra of discharge sources in xenon and tin: comparison of computer simulations and experimental results



E.R. Kieft¹, K. Garloff¹, J.J.A.M. van der Mullen¹, V. Banine²

¹Eindhoven University of Technology, P.O. Box 513, 5600 MB Eindhoven, The Netherlands

²ASM Lithography B.V., P.O. Box 325, 5500 AH Veldhoven, The Netherlands

Introduction and Motivation

Discharge plasmas are candidates for EUV light sources in future lithography systems; commonly used working elements xenon and tin produce broad spectra consisting of 'quasi-continuum' bands rather than sharp peaks.

- Out-of-band parts of the spectrum have an effect on the heating of optics;
 - Absolute and relative intensity data over large ranges are needed for comparison with output of modeling.
- Need for calibration of spectrometer sensitivity

Spectral modeling is desired for better understanding (and hopefully better control) of the physical properties of the plasma. Problem with existing model(s): unlike for laser produced plasmas, certain equilibrium assumptions (LTE, steady-state ion distribution) may not be valid in EUV discharge plasmas.

→ Need for a model that incorporates such non-equilibrium behaviour

This poster: describes comparison of **sensitivity-corrected** experimental EUV spectra with output from a dedicated **computer model**

The following experimental spectra were selected for comparison with computer simulations:

- Xenon:** spatially integrated, time-resolved spectra [1] from a Philips HCT discharge [2] recorded from axial position at 20, 10 and 0 ns before the pinch → spectra (a) to (c)
- Tin:** space- and time resolved spectra [3] from a vacuum arc discharge in tin vapor from ISAN recorded from a position perpendicular to the axis, ~0.1 to 0.45 mm from cathode 40, 20 and 0 ns before pinch → spectra (d) to (f)

The simulation input parameters were varied by hand to match the simulated spectra to experimental results.

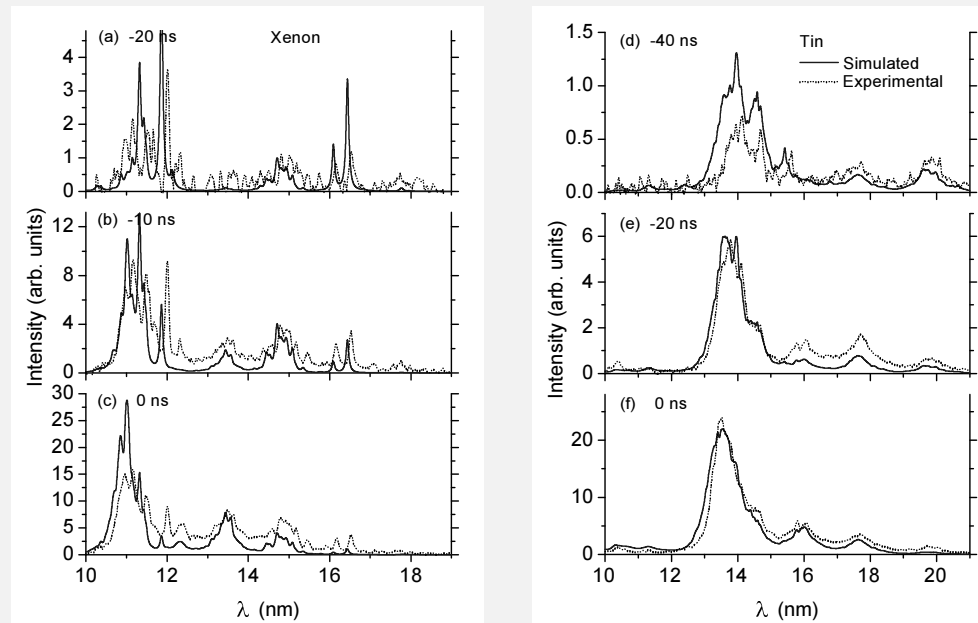


Fig. 3: Comparison of simulated and experimental spectra for xenon (left) and tin (right) discharges. Dotted curves represent (sensitivity corrected) experimental results, while solid curves represent simulations. Within each set of results, the units and the intensity ratios between simulated and experimental spectra were kept fixed. Spectra names (a) to (f) are defined in the text to the left and below.

The spectral model

- Based on the radiation module of an LPP simulation model by Garloff et al. [7]
- Calculates ion distribution (and n_e), excited state densities, and emitted EUV radiation from $n_{i,tot}$, T_e , and size and geometry of the plasma
 - Incorporates v_i as an additional input parameter, accounting for a net ionization rate (defined as imbalance between ionization and recombination rates)
 - Natural, Doppler and Stark broadening effects
 - Opacity: exponential approach of Planck level for each wavelength of radiation
 - Fully analytical Collisional Radiative Model (based on the work in [8]) for state distribution functions of ions and excited states (see Fig. 2):
 - Ionization rate: sum of direct ionization and collisional excitation from ground state into all levels that are in 'hot' Excitation Saturation Balance (ESB) (note: excitation into first ESB level contributes by far the most)
 - Excited state densities: combination of Corona and ESB

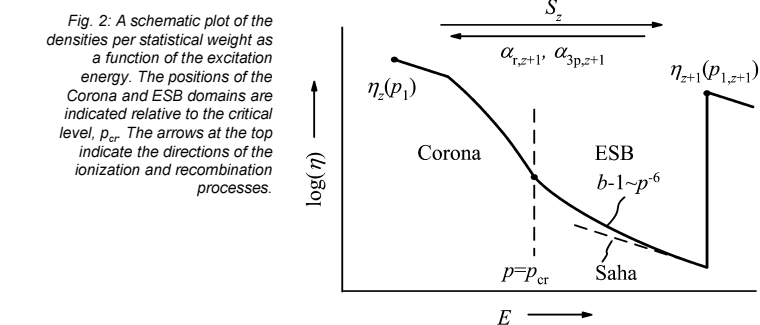


Fig. 2: A schematic plot of the densities per statistical weight as a function of the excitation energy. The positions of the Corona and ESB domains are indicated relative to the critical level, p_{cr} . The arrows at the top indicate the directions of the ionization and recombination processes.

• Detailed atomic data for Xe, Sn^{8+–12+} from calculations using the Cowan code [9]

Spectrometer sensitivity calibration

The spectrometer applied for the experimental results as used here, is a grazing-incidence 1 m reflection spectrometer i.c.w. a multichannel plate (MCP) detector in off-Rowland circle configuration.

Factors that influence spectrometer efficiency:

- Geometrical efficiency of the grating (reflection into 1st order) 1200 l/mm ruled grating, 1° blaze angle, coated with a 60 nm layer of gold
 - Grazing-incidence reflectivity of gold [4]
 - Inverse wavelength dispersion on MCP detector surface
 - Photocathode efficiency of Au front-coated MCP
- The latter should be evaluated for a 'contaminated' Au surface [5].

Experimental calibration was performed through comparison with photodiode signals from a Flying Circus tool [6], using ML mirrors designed for different wavelength bands.

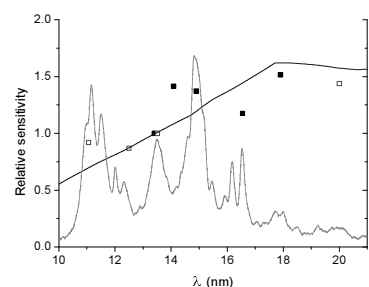


Fig. 1: Theoretical (solid line) and measured (square blocks) spectrometer sensitivities as a function of wavelength. An experimentally obtained xenon spectrum (dotted line) has been included for reference.

Reasonable agreement has been found between the theoretical curve and experiments (see Fig. 1). The theoretical curve has been applied for correction of experimental spectra.

Results

Experimental and simulated spectra are shown together in Fig. 3. For spectra (b) and (e), Fig. 4 shows the contributions of the various individual ions to the simulated spectra.

The optimized input parameters for the simulations and certain characteristics of the results are summarized in Table I.

Comparison of total in-band output in simulations with absolute output data from Flying Circus measurements:

- xenon: 25 mJ in-band (over 4π) measured vs. 2.0 mJ in 5 ns, for a ~50 ns EUV pulse
- tin: 60 mJ vs. 6.8 mJ in 5 ns, for a ~30 ns pulse.

Name	n_i (10^{23} m^{-3})	T_e (eV)	v_i (10^7 s^{-1})	r (mm)	l (mm)	Z_{av}	n_e (10^{25} m^{-3})	I_{tot} (mJ)
Xe (a)	1.35	24.5	4	0.55	1	8.32	0.112	3.0
Xe (b)	2.6	27	4.5	0.4	1	9.18	0.24	10.1
Xe (c)	10	25.5	1	0.2	1	9.86	0.99	24
Sn (d)	0.78	24	1.5	0.7	0.5	8.54	0.067	2.3
Sn (e)	3.1	23	3	0.35	0.5	9.21	0.29	9.1
Sn (f)	31.5	23	5	0.11	0.5	9.73	3.1	38

Table I: Input parameters and simulation results; n_i – total ion density; T_e – electron temperature; v_i – net ionization rate; r, l – plasma radius, length; Z_{av} – average ion charge; n_e – electron density; I_{tot} – total energy radiated in EUV in 5 ns time.

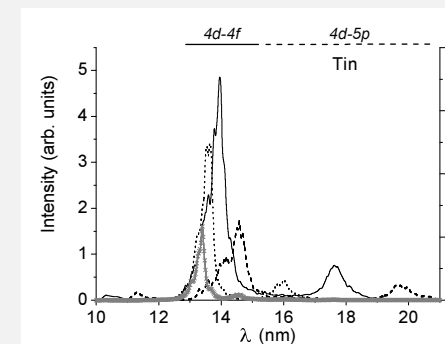
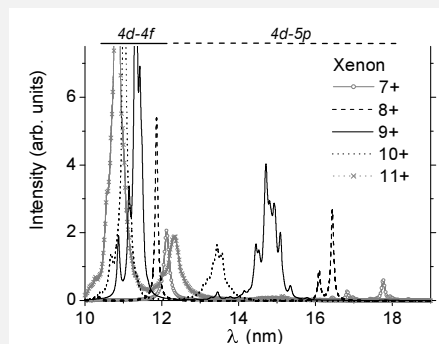


Fig. 4: Contributions of the different ions to the overall spectra (b) (xenon, left) and (e) (tin, right). For both graphs: 7+ - grey curve with open circles; 8+ - dashed curve; 9+ - solid curve; 10+ - dotted curve; 11+ - grey curve with crosses. The Xe⁷⁺ and Xe¹¹⁺ curves have been magnified 15x to make them visible on the same scale; the Sn¹¹⁺ plot has been magnified 2 times in comparison with the other plots. The solid overbars indicate the positions of the 4d-4f transitions of the various ions; the 4d-5p transitions are indicated by the dashed bars.

Discussion and conclusions

A fairly good agreement has been obtained between experiments and simulations on the parts of

- Shapes and positions of individual features (related to output of atomic data calculations)
- Absolute intensities of the spectra
- Relative intensities of 4d-4f vs. 4d-5p features (thanks to spectrometer sensitivity correction, application of a CRM, and detailed treatment of line broadening / opacity)

Remaining differences between simulation and experiment may follow from, among others:

- Limitation in the number of excited levels and lines that could be included (e.g. no doubly excited states)

- Homogeneous plasma assumption:
 - no additional absorption due to cooler plasma on the outside
 - no mixing of spectra from regions/phases with different plasma parameters

Further improvements would probably require calculation of excited state densities based on detailed information on rates, rather than on analytical expressions that depend on energy only.

Realistic values were applied for all relevant parameters. Where numbers can be compared, they are in reasonable agreement with other diagnostics (a.o. Thomson scattering). Specifically, a realistic value for v_i is combined with relatively low T_e → The results seem to indicate that there is *no need to assume very high T_e* to compensate for ionization imbalance.

A full publication of the method and the results is planned for the near future.

References

1. E.R. Kieft, J.J.A.M. van der Mullen, G.M.W. Kroesen, and V. Banine, Phys. Rev. E **68**, 056403 (2003).
2. K. Bergmann, G. Schriever, O. Rosier, M. Müller, W. Neff, and R. Lebert, Appl. Opt. **38**, 5413 (1999).
3. E.R. Kieft, J.J.A.M. van der Mullen, G.M.W. Kroesen, V. Banine, and K. Koshelev, to be published.
4. http://www-cxro.lbl.gov/optical_constants/.
5. H. Henneken, F. Scholze, M. Krummy, and G. Ulm, Metrologia **37**, 485 (2000).
6. R. Stuik, H. Fledderus, P. Hegeman, J. Jonkers, M. Visser, V. Banine, and F. Bijkerk, in Proceedings of the 2nd SEMATECH Workshop on Extreme UV Lithography, San Francisco, 2002.
7. K. Garloff, M. van den Donker, J.J.A.M. van der Mullen, F. van Goor, R. Brummans, and J. Jonkers, Phys. Rev. E **66**, 036403 (2002).
8. J.J.A.M. van der Mullen, Phys. Rep. **191**, 109 (1990).
9. R.D. Cowan, *The theory of atomic structure and spectra* (Univ. of California Press, Berkeley, 1981).